(4)

OFFICE OF NAVAL RESEARCH

Contract N00014-80-K-0852

R&T Code_____

Technical Report No. 45

Understanding Core Level Decay Processes In the High-Temperature Superconductors

By

D. E. Ramaker, N. H. Turner and F. L. Hutson

Prepared for Publication

in the

Physical Review B

George Washington University
Department of Chemistry
Washington, D.C. 20052

December, 1988

ADA202078

SECURITY CLASSIFICATION OF THIS PAGE

REPORT DOCUMENTATION PAGE

1a. REPORT SECURITY CLASSIFICATION Unclassified	1b. RESTRICTIVE MARKINGS
2a. SECURITY CLASSIFICATION AUTHORITY	3. DISTRIBUTION/AVAILABILITY OF REPORT Approved for Public Release, distribution Unlimited.
2b. DECLASSIFICATION/DOWNGRADING SCHEDULE	
4. PERFORMING ORGANIZATION REPORT NUMBER(S) Technical Report # 45	5. MONITORING ORGANIZATION REPORT NUMBER(S)
6a. NAME OF PERFORMING ORGANIZATION Dept. of Chemistry George Washington Univ. 6b. OFFICE SYMBOL (If applicable)	7a. NAME OF MONITORING ORGANIZATION Office of Naval Research (Code 413)
6c. ADDRESS (City, State, and ZIP Code) Washington, D.C. 20052	7b. ADDRESS (City, State, and ZIP Code) Chemistry Program 800 N. Quincy Street Arlington, VA 22217
8a. NAME OF FUNDING/SPONSORING ORGANIZATION Office of Naval Research 8b. OFFICE SYMBOL (If applicable)	9. PROCUREMENT INSTRUMENT IDENTIFICATION NUMBER Contract N00014-80-K-0852
8c. ADDRESS (City, State, and ZIP Code) Chemistry Program 800 North QUINCY, Arlington, VA 22217	10. SOURCE OF FUNDING NUMBERS PROGRAM ELEMENT NO. 61153 N; PROJECT NO.; TASK NO. PP 013-08-01; WORK UNIT ACCESSION NO NR 056-681
11. TITLE (Include Security Classification) Understanding Core Level Decay Processes in the High-Temperature Superconductors (Uncl.)	
12. PERSONAL AUTHOR(S) D. E. Ramaker, N. H. Turner, and F. L. Hutson	
13a. TYPE OF REPORT Interim Technical 13b. TIME COVERED FROM _____ TO _____	14. DATE OF REPORT (Year, Month, Day) December 1988 15. PAGE COUNT 10
16. SUPPLEMENTARY NOTATION Prepared for publication in Physical Review B	
17. COSATI CODES FIELD / GROUP / SUB-GROUP	18. SUBJECT TERMS (Continue on reverse if necessary and identify by block number) Superconductivity, Auger Spectroscopy, X-ray Emission Spectroscopy, Hubbard Model, Copper Oxides

19. ABSTRACT (Continue on reverse if necessary and identify by block number)

A highly correlated CuO_n cluster model is utilized to interpret the core level Auger and X-ray emission decay spectra for $YBa_2Cu_3O_{7-y}$ and CuO. The evidence indicates that the initial-state shakeup states relax to states of the same symmetry before the core level decay, provided they have a shakeup excitation energy much greater than the core level width.

20. DISTRIBUTION/AVAILABILITY OF ABSTRACT ☐ UNCLASSIFIED/UNLIMITED ☒ SAME AS RPT. ☐ DTIC USERS	21. ABSTRACT SECURITY CLASSIFICATION Unclassified
22a. NAME OF RESPONSIBLE INDIVIDUAL Dr. David L. Nelson	22b. TELEPHONE (Include Area Code) (202) 696-4410 22c. OFFICE SYMBOL

DD FORM 1473, 84 MAR — 83 APR edition may be used until exhausted. All other editions are obsolete.

SECURITY CLASSIFICATION OF THIS PAGE
Unclassified

(1)

Previously reported [1,2] core level Auger (AES) and x-ray emission (XES) data are interpreted within a highly correlated CuO_6 cluster model for the high-temperature superconductors (HTSC's), $YBa_2Cu_3O_{7-z}$ and $La_{2-x}Ba_xCuO_4$ (herein referred as 123 and La). The $L_{23}M_{23}V$ Auger lineshape is reported here for the first time and is interpreted consistently with the $L_{23}VV$ lineshape and XES data. This work clearly indicates, contrary to previous reports [1,3], that the initial-core shake-up (ICSU) states do not directly decay, but rather relax to the primary core-state before decay. The XES data dramatically reveal the change of character of the valence band (VB) states between CuO and 123.

The basic electronic structure of the HTSC's can be described by an extended Hubbard model, characterized by the transfer or hopping integral t, the Cu and O orbital energies ϵ_d and ϵ_p, the *core polarization energy* Q_d, the intra-site Coulomb repulsion energies U_d and U_p, and the inter-site repulsion energies U_{dp} and U_{pp} (i.e. between neighboring Cu-O and O-O atoms). The extended Hubbard model is most appropriate when the U's are large relative to the band widths [3], i.e. when correlation effects dominate covalent or hybridization effects. A $CuO_n^{(2n-2)-}$ cluster model, which is also reasonably valid when U >> t, simplifies the model [3]. Both La and CuO contain CuO_6 groups [4], having 4 *short* and 2 *long* Cu-O bonds. The 123 HTSC contains CuO_5 and planar CuO_4 groups [4]. The different n may alter the relative intensities of various features, but similar features are present in each case. The different bond lengths may increase the widths of the spectral features, but little else since correlation dominates.

The $CuO_n^{(2n-2)-}$ cluster has one hole shared between the Cu 3d and O 2p shells in the ground state, which we term the v (valence) states. The spectroscopic final states reflect multi-hole states, e.g. v^2, cv (c = core) etc.

We indicate the location of the v holes by d (Cu 3d) or p (O 2p). In the case of two holes on the oxygens, we distinguish two holes on the same O (p^2), on ortho neighboring O atoms (pp^o), or on para O atoms (pp^p) of the cluster. Furthermore, neighboring pp^o holes can dimerize [5], so we distinguish between two holes in bonded (pp^o_b) and antibonded (pp^o_a) O pairs. Most of the O atoms actually participate in two CuO_2 clusters. Consistent with previous work [6], we account for this by defining the effective parameter, $\epsilon_p = \epsilon_p' + U_{pe}$, where U_{pe} includes the interaction of a hole in an O p orbital with its environment. In general U_{pe} will be less than U_{dp} due to polarization.

The v states, as reflected by the theoretical DOS [7], can be described as having the Cu-O bonding (ψ_b) and antibonding (ψ_a) orbitals centered at 4 and 0 eV and the nonbonding Cu and O orbitals at 2 eV. The O features each have a width 2Γ = 4 eV due to the O-O bonding and antibonding character and the Cu-O dispersion. The ψ_b and ψ_a wavefunctions can be expressed as [3],

$$\psi_a = d\cos\vartheta_1 - p\sin\vartheta_1 \qquad (1a)$$

$$\psi_b = d\sin\vartheta_1 + p\cos\vartheta_1, \qquad (1b)$$

where $\vartheta_1 = 0.5\tan^{-1}(2t/\Delta)$. We also define the Cu-O hybridization shift $\delta_1 = 0.5\,\mathrm{sqrt}(\Delta^2+4t^2) - \Delta/2$, which is utilized in Table 1 to give the energies. In this picture, the ground state of an average CuO_2 cluster is located at 1 eV having the energy $\epsilon_d-\delta_1+\Gamma/2 = \epsilon_d-\alpha$, which we use as a reference energy for the excited v^2, v^3, and cv states reflected in the core level spectra. In CuO, the hybridization shift Γ is smaller, and we shall see below that $\Delta=\epsilon_p-\epsilon_d$ has increased to 1 eV.

Recently [8] we consistently interpreted the VB photoelectron spectra (UPS and XPS). Most of the features in the UPS and XPS are also reflected

in the AES and XES, so that we review these assignments here. In 123, the states were assigned as indicated in Table 1 [8,10]. Calculated photoemission intensities, their variation with Δ, and photon energy dependencies confirm these assignments [8]. In CuO [9], we have previously assigned a feature at 5.5 eV to pp^{e}_{s} and pp^{s} and at 3 eV to dp. The character switch of state 1 from mostly dp to pp^{s} and vice versa for state 2 between CuO and 123 arises because Δ decreases from 1 eV in CuO to 0 eV in 123. The reduction in Δ as indicated by the UPS data is consistent with the Cu 2p XPS data and with the XES data to be discussed below.

The "shakeup" or "many-particle" features at 9.5, 12.5, and 16 eV have also been assigned as indicated in Table 1 [8]. The pp^{e}_{b} state has been assigned to the "mystery" feature at 9.5 eV. Such a feature also appears for CuO [9,11] so that this feature is not unique to the HTSC's. This feature cannot arise from the p^2 final state because U_p is around 12-13 eV, much too large to cause a feature at 9.5 eV. In fact we have found evidence [8] for the existence of the p^2 feature around 16 eV in 123. Finally the d^2 state is known to cause the 12.5 eV feature [12].

Cu 2p and O 1s core level XPS. In order to understand the XES and AES data, we first characterize the initial state, which is reflected directly in the Cu 2p and O 1s XPS data. The primary and satellite features seen in the Cu 2p XPS spectrum for CuO [13] and 123 or La [1,14] are known to arise from the cp and cd states, respectively [3], having the energies given in Table 1. The relative satellite intensity, I(cp)/I(cd) decreases from 0.55 in CuO to 0.37 in 123 as determined from the experimental data [1]. The energy separation, E(cd) - E(cp) increases from 8.7 eV in CuO to 9.2 in 123 [1].

The primary (cp) and satellite (cd) wavefunctions can be written similar to eq. (1), with hybridization angle $\vartheta_c = 0.5 \tan^{-1}(2t/(\Delta - Q_d))$ [3]. In the

sudden approximation, the intensities are proportional to the overlap between the ground state wavefunction, ψ_g, and the final states, so that $I(dp) \propto \cos^2(\vartheta_c-\vartheta_1)$ and $I(cd) \propto \sin^2(\vartheta_c-\vartheta_1)$ [3]. Thus the satellite intensity increases with change in the hybridization angles between the v and cv states. In the ground v state, the hole is shared equally in the p and d orbitals since j1 ? 45°, in the primary cv state it is mostly in the p orbital since jc ? 78°. The changes between CuO and 123 noted above are just that expected for a decrease in Δ and reflect an increased covalency in 123 [15].

The large width of the primary cp peak is believed to arise from the mixing with the cd state [3,15]. The cd state has a large width due to the large core-hole, valence-hole interaction, indeed, the satellite actually reveals the cd multiplet structure. Evidence that the primary cp peak width arises from the cd interaction comes from the Cu halide data [3], which show a direct correlation of the primary cp peak width with the satellite cd peak intensity. We do not believe that the primary peak width arises from the O p band width as proposed by others [16].

The O 1s spectra have been reported by many authors; however, it is seriously altered by impurities such as OH^- and $CO_3^=$ on the sample surface [17]. Recent data [18] from single crystal samples of the La material cleaved in-situ are expected to be reasonably free of impurity effects. The cp^a and cp^b states listed in Table 1 are believed to account for the tailing off of the spectra seen in these spectra (this will be positively identified upon examination of the XES data). Consistent with the sudden approximation, the cp state is not seen in the O 1s XPS because now both the v and cv states have similar hybridization angles, i.e. the valence hole is mostly in the d orbital in both cases.

We will find below that the ISSU process, which is responsible for the satellites in the XPS noted above, does not produce satellites in the AES or XES data, because the ISSU states generally "relax" to the primary states of the same symmetry before the core level decay. Such a relaxation is expected when the ISSU excitation energy is larger than the core level width [19].

Previously, vanderLaan et al [3] suggested the intensity of these ISSU states in the XPS should be quantitatively reflected in the intensity of the Auger satellites found in the $L_{23}VV$ lineshapes for the Cu halides. The data do not indicate this however. While I(cd)/I(cp) increases from 0.45 for $CuBr_2$ to 0.8 for CuF_2, the Auger satellites do not increase [3]. We previously [1] indicated that a fraction of these ISSU states probably resulted in Auger satellites for the HTSC's, and that this fraction increased with the increasing covalency of the HTSC material. Evidence presented here indicates rather that the ISSU states relax before the core level decay to states of the same symmetry, provided they have a ISSU excitation energy much greater than the core level width. We believe this to be a general result, at least in the Cu^{+2} materials.

<u>The Cu L_{23} and O K XES data</u>. The O K XES data [2] in Figure 1a confirms our assignment of the O XPS, and clearly shows the dependency of the ISSU state relaxation on the excitation energy and symmetry. The principal XPS peak arises from the cd state, and it decays to the dp state since the x-ray emission process is intra-atomic in nature. Therefore the principal O XES peak aligns with the dp feature in the UPS as shown in Fig. 1. The cp^6 state does not mix with the primary cd state; therefore, it does not relax before the decay, but decays directly to the pp^6_b (and perhaps a little also to the pp^6_a) state. This accounts for the feature around 6.5 eV in the XES, just 3 eV above the pp^6_b feature in the UPS. The shift of 3 eV matches the energy

difference between the cp^6 and cd core hole states. The cp^5 state can mix with the cd state, therefore it can relax to the cd state, but it does this slowly because of the small excitation energy of 0.5 eV. Therefore, the cp^5 state decays either directly to the pp^5 state, or relaxes to the cd state, which then decays to the dp state. This explains the photon energy dependence seen [2] in the data of Fig. 1a. At high photon energy, the sudden approximation is more valid, creating a larger intensity for the cp^5 state, and consequently a larger pp^5 contribution around 2.5 eV in the XES.

The Cu L_{23} XES data [2,20] shown in Figure 1b dramatically reveals the switch in character of the 1 and 2 v^2 states between CuO and 123. Again, the satellite cd initial state relaxes to the cp state before the decay so that the XES reflects primarily the dp DOS. In CuO the XES spectrum peaks at 3 eV, in 123 it falls around 4.2 eV, very near where we indicated the dp states fall in the UPS data. The large intensity in the CuO XES extending above the Fermi level is believed to be an experimental artifact [20].

The Cu $L_{23}VV$ and $L_{23}M_{23}V$ Auger data. Comparison of the L_3VV data for CuO [11] and 123 [1] are shown in Fig. 2. The data reveal features at 7 (the two-center feature), 15, and 19 eV, which we previously [1] attributed to dp, d^2, and d^3 final states, utilizing a v^2 final state model. The d^3 states were attributed to a combination of 3 different processes; 1) initial state shakeoff (ISSO) followed by Auger decay (g.s. + $h\nu \rightarrow L_3v \rightarrow d^3$), 2) Coster-Kronig (CK) decay followed by Auger decay (g.s. + $h\nu \rightarrow L_{12} \rightarrow L_3v \rightarrow d^3$), and 3) ISSU followed by Auger decay (g.s. + $h\nu \rightarrow L_3ve \rightarrow L_3v \rightarrow d^3$, where e denotes the excited electron). The ISSO and CK processes accounted for all of the d^3 component in CuO, and the ISSU process was believed, as mentioned above,to account for the increasing d^3 component in La and 123 [1].

We report and interpret here, for the first time, the $L_{23}M_{23}V$ Auger

lineshapes for the 123 SC. The sample preparation, treatment, and instrument utilized were described previously [1]. Fig. 2 compares the $L_{23}M_{23}V$ spectra for CuO [[24] and 123 , and identifies the various features. The $L_{23}M_{23}V$ lineshapes reflect the cv^2 DOS, the main features arising from the cdp final state, and the satellite from the cd^2p state apparently resulting from the similar ISSO, CK, and ISSU processes defined above. However, Fig. 2 reveals a most interesting point; although 123 shows an increased satellite in the $L_{23}VV$ relative to CuO, it is not increased in the $L_{23}M_{23}V$. This indicates strongly that the ISSU process is not responsible for the increased satellite in the L_3VV, because then it should increase the satellite in both 123 lineshapes.

Since only the primary cp core-hole state Auger decays, and this process is also known to be strictly intra-atomic, the $L_{23}VV$ lineshape in our current v^3 final state model, reflects the d^2p DOS, as it is distributed among the v^3 states listed in Table 1. Thus the features at 7, 15, and 19 eV arise naturally from the dpp^p, d^2p, and dp^2 final states. The ISSO and CK processes also contribute to the "satellite" contribution at 19 eV just as in CuO. The dpp^o state does not appear in the L_3VV lineshape because it does not have the same symmetry possessed by all the other v^3 final states and the cv initial state. The increased "satellite" feature at 19 eV in the HTSC's arises apparently because of increased configuration mixing between the d^2p and dp^2 states. Its intensity is increased in 123 relative to CuO because the energy separation (before hybridization) between d^2p and dp^2 has decreased from 3.8 eV in CuO to 2.5 eV in 123. We have indicated this mixing in Table 1 by adding the hybridization shifts δ_2 to the energy expressions for these two states.

The $L_{23}M_{23}V$ lineshape reflects the cdp DOS. The mixing of the other states (cd^2, cpp^p, cpp^o_a, and cpp^o_b; the latter three are not listed in Table 1)

with the cdp state is small because of the large energy separations involved. The cp^2 state is close to cdp; however, it falls in between the ^3L and ^1L multiplets of the cdp state. Although it may have some intensity, it surely does not contribute to the CK + SU satellite around 25 eV in either CuO or 123. The exchange splitting (2K) between the 3p and d holes is known to be very large [3], so we include it explicitly in Table 1 to account for the $^{1,3}L$ multiplets.

The O KVV lineshape is severely altered by impurities on the sample surfaces, and no single crystal lineshape data have been reported. The O KVV lineshapes for CuO and Cu_2O have been reported [11], and they have the primary dp^2 or p^2 features, respectively, around 19 eV. A very small satellite appears around 7 eV in Cu_2O which we attribute to the pp^2 state. A much larger and broader satellite around 7 to 14 eV in CuO appears, which we attribute to the d^2p state around 14 eV as well as a smaller amount to the dpp^2 state around 7 eV. Thus the d^2p and dp^2 states appear in both the Cu $L_{2,3}VV$ and O Auger lineshapes for Cu^{+2} oxides, except their primary and satellite roles are reversed.

In summary, we have interpreted XES and AES data utilzing a highly correlated CuO_8 cluster model. Both the XES data and the previously interpreted UPS data reveal the reversal in character of the VB states between CuO and the HTSC's. We have also shown that the initial-state shake-up states evident in core level XPS, do not generally produce satellites in the core emission spectra, because they relax to the primary core states of the same symmetry, provided the ISSU excitation energy is greater than the core level width.

TABLE 1 Summary of hole states revealed in the spectroscopic data, and estimated energies using the following optimal values for the Hubbard parameters in eV[a]:

δ_1 = 2	ϵ_d = 2	U_p = 12, 13	U_d =9.5,10.2
δ_2 = 0.5,0.8	ϵ_p = 2, 3	U_{pp}° = 4.5, 4	U_{dp} =1
Γ = 2	U_{pp}[b] = 0.	U_{cp}° = 2	Q_d =9
α = 1, 0.5	Δ = 0, 1.	K= 4	

State[b]	Energy expression	Calc. E. eV[c,d]	Exp. E. eV[c]	Remark
G.S. and IPES, v^0				
^{1}a) d	$\epsilon_d - \delta_1 \mp \Gamma$	0 ∓ 2	-	heavily
^{3}a) p	$\epsilon_p + \delta_1 \mp \Gamma$	4 ∓ 2	-	mixed
UPS and XES, v^2				
1)° pp[b]	$\epsilon_p + \Delta - \delta_2 + \alpha$	2.5	2.5	heavily
2)° dp	$\epsilon_p + U_{dp} + \delta_2 + \alpha$	4.5	4.2	mixed
3) pp°[a]	$\epsilon_p + \Delta + U_{pp}$° $- \Gamma + \alpha$	5.5	5.	
4) pp°[b]	$\epsilon_p + \Delta + U_{pp}$° $+ \Gamma + \alpha$	9.5	9.5	mystery peak
5) d^2	$\epsilon_d + U_d + \alpha$	12.5	12.5	Cu sat.
6) p^2	$\epsilon_p + \Delta + U_p + \alpha$	15	16	
Cu 2p XPS, cv				
cp	$\epsilon_c + \Delta + \alpha$	ϵ_c + 1	E_{2p}	main
cd	$\epsilon_c + Q_d + \alpha$	ϵ_c + 10	E_{2p}+9.2	sat.
O 1s XPS, cv				
cd	$\epsilon_c + \alpha$	ϵ_c + 1	E_{1s}	main
cp[b]	$\epsilon_c + \Delta + \alpha$	ϵ_c + 1	E_{1s}	main
cp°	$\epsilon_c + \Delta + U_{cp}$° $+ \alpha$	ϵ_c + 3	E_{1s}+2 ?	tail
cp	$\epsilon_c + \Delta + Q_p + \alpha$	?	?	not obs
Cu L_3VV AES, v^2				
dpp[b]	$2\epsilon_p + 2U_{dp} + \alpha$	7	7	2 cent. feature
dpp°	$2\epsilon_p + U_{pp}$° $+ 2U_{dp} + \alpha$	11.5	-	no mixing
d^2p	$\epsilon_d + \epsilon_p + U_d + 2U_{dp} - \delta_2 + \alpha$	16	15.5	main feature
dp^2	$2\epsilon_p + U_p + 2U_{dp} + \delta_2 + \alpha$	19.5	18-25	sat. feature
Cu $L_3M_{2,3}V$ AES, cv^2				
cdp	$\epsilon_c + \epsilon_p + Q_d + U_{dp} \mp K + \alpha$	ϵ_c +9	E_{2p}+10	main, ^{1}L
		ϵ_c+17	E_{2p}+18	main, ^{3}L
cp^2	$\epsilon_c + \epsilon_p + \Delta + U_p + \alpha$	ϵ_c + 15	-	not observed
cd^2	$\epsilon_c + \epsilon_d + U_d + 2Q_d + \alpha$	ϵ_c+30.5	-	not observed

[a]Parameters for 123 indicated first, those for CuO second.
[b]The dominant character in the hybridized states is given.
[c]The Calc. E and Exp. E columns indicate the results for 123.
[d]The calculated E is defined relative to the ground v^1 (d) state energy = ϵ_d - α. The v^1(d) energy defines the Fermi level relative to the vacuum level at zero.
[e]The dominant character switches as described in the text, and thus the sign in front of δ_2 is the opposite for CuO.

Figure Captions

Fig. 1a) Comparison of O K XES data for 123 taken at the indicated photon excitation energies (from Ref.2).

1b) Comparison of Cu L_{23} XES data for 123 (Ref. 2) and CuO (Ref. 20).

1c) UPS data for 123 ($h\nu$ = 74 eV from Ref. 10).

Fig. 2) Comparison of Auger data for the materials indicated. Cu $L_{23}VV$ data for CuO and 123 from refs. 25 and 1. Cu $L_{23}M_{23}V$ data for CuO from ref. 24 and for 123, this work. The $L_{23}VV$ data is on a 2-hole binding energy scale = E_{L3}-$E_{k,,}$ and the $L_{23}M_{23}V$ on a 1-hole scale = E_{L3}-E_k-E_{N3}, where E_{L3} = 933.4 and E_{N3} = 77.3 eV [9,11].

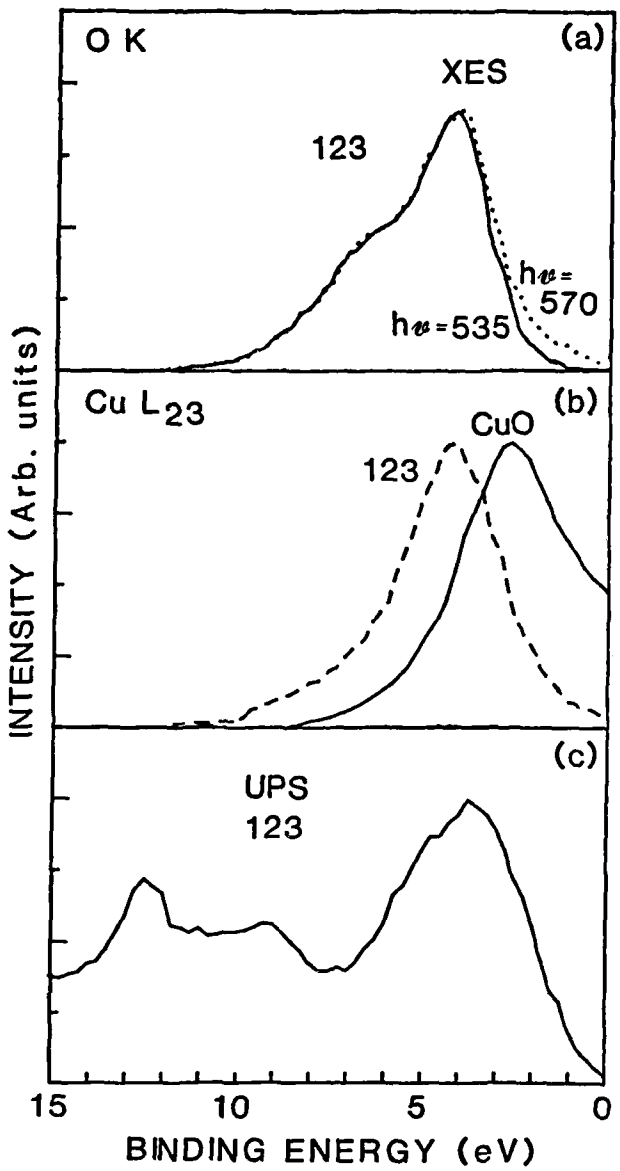
O K
(a)
XES
123
hν=
570
hν=535
Cu L23
(b)
CuO
123
(c)
UPS
123
INTENSITY (Arb. units)
15
10
5
0
BINDING ENERGY (eV)

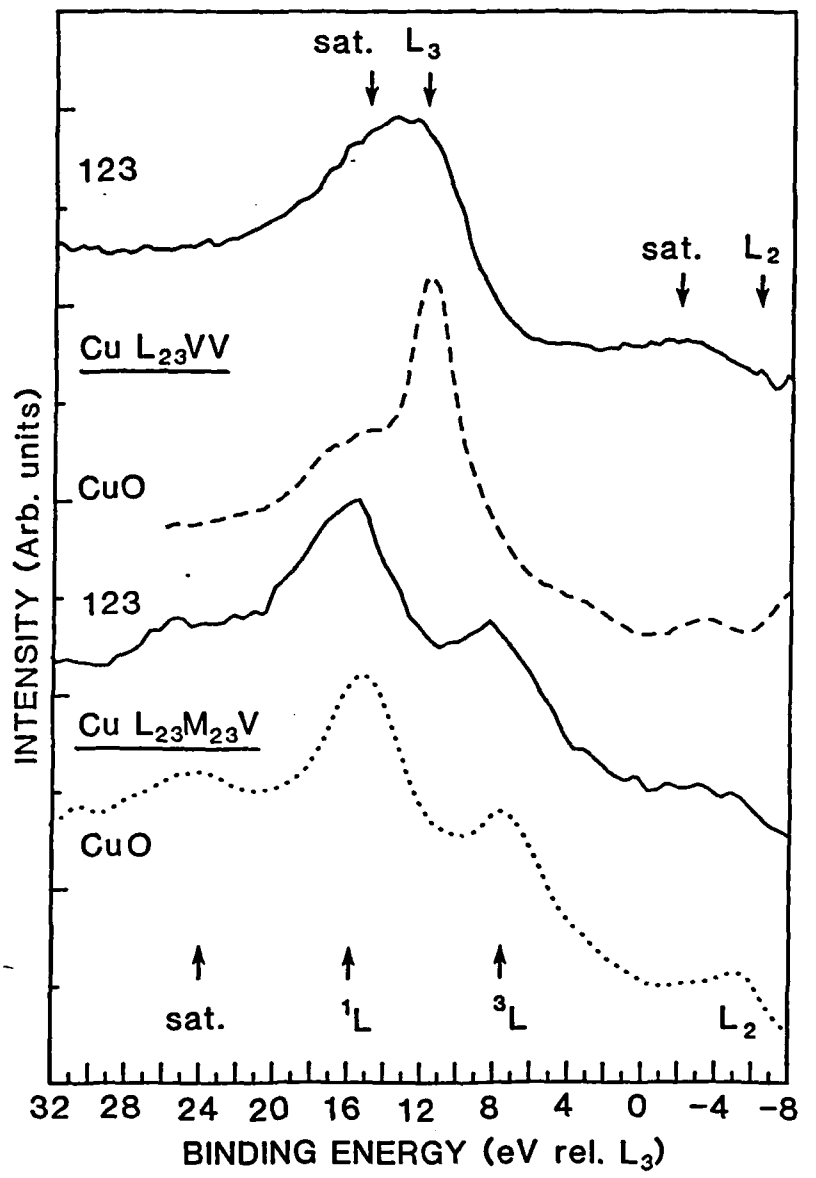
sat. L3
123
sat. L2
Cu L23VV
CuO
123
Cu L23M23V
CuO
sat.
1L
3L
L2
INTENSITY (Arb. units)
32 28 24 20 16 12 8 4 0 −4 −8
BINDING ENERGY (eV rel. L3)

References

1. D.E. Ramaker et al., Phys. Rev. 36, 5672 (1987).
2. K.L. Tsang et al., Phys. Rev. B37, 2293 (1988).
3. G. vanderLaan et al., Phys. Rev. 24, 4369 (1981); J.C. Fuggle et al., Phys. Rev. B37, 1123 (1988).
4. J.E. Greedan et al., Phys. Rev. B35, 8770 (1987).
5. R.A. de Groot, H. Gutfreund, and M. Weger, Sol. State Commun. 63, 451 (1987); W. Folkerts et al., J. Phys. C: Solid State Phys. 20, 4135 (1987); A. Manthiram, X.X. Tang, and J.B. Goodenough, Phys. Rev. B37, 3734 (1988).
6. J.E. Hirsch et al., Phys. Rev. Letters 60, 1168 (1988).
7. J. Redinger et al., Phys. Lett. 124, 463 and 469 (1987).
8. D.E. Ramaker, N.H. Turner, and F.L. Hutson, submitted.
9. M.R. Thuler, R.L. Benbow, and Z. Hurych, Phys. Rev. B26, 669 (1982).
10. N.G. Stoffel et al., Phys. Rev. B37, 7952 (1988); also preprint.
11. C. Benndorf et al., J. Electron. Spectrosc. Related Phenom. 19, 77 (1980).
12. R. Kurtz et al., Phys. Rev. B35, 8818 (1987).
13. A. Rosencwaig and G.K. Wertheim, J. Elect. Spectrosc. Related Phenom. 1, 493 (1972/73).
14. P. Steiner et al., Z. Phys. B- Condensed Matter 67, 497 (1987).
15. D.E. Ramaker et al., Phys. Rev. 36, 5672 (1987).
16. D.D. Sarma, Phys. Rev. B37, 7948 (1988).
17. S.L. Qiu et al., Phys. Rev. B37, 3747 (1988); W.K. Ford et al., Phys. Rev. B37, 7924 (1988); D.E. Ramaker, N.H. Turner, and F.L. Hutson, In Thin Film Processing and Characterization of High Temperature

Superconductors, J.M.Harper, J.H. Colton, and L.C. Feldman eds., AVS Series No. 3 (American Institute Physics, New York, 1988), p 284.

18. T. Takahashi et al., Phys. Rev. B37, 9788 (1988).

19. J.W. Gadzuk and M. Sunjic, Phys. Rev. B12, 524 (1975).

20. A.S. Koster, Mole. Phys. 26, 625 (1973).

21. D. van der Marel et al., Phys. Rev. B37, 5136 (1988).

22. Y. Chang et al., Phys. Rev. B (In press).

23. N. Nucker et al., Z. Phys. B: Cond. Matter 67, 9 (1987); Phys. Rev. 37, 5158 (1988).

24. L. Fiermans, R. Hoogewijs, and J. Vennik, Surf. Sci. 47, 1 (1975).

25. P.E. Larson, J. Electron Spectrosc. Related Phenom. 4, 213 (1974).

DL/1113/87/2

TECHNICAL REPORT DISTRIBUTION LIST, GEN

	No. Copies
Office of Naval Research Attn: Code 1113 800 N. Quincy Street Arlington, Virginia 22217-5000	2
Dr. Bernard Douda Naval Weapons Support Center Code 50C Crane, Indiana 47522-5050	1
Naval Civil Engineering Laboratory Attn: Dr. R. W. Drisko, Code L52 Port Hueneme, California 93401	1
Defense Technical Information Center Building 5, Cameron Station Alexandria, Virginia 22314	12 high quality
DTNSRDC Attn: Dr. H. Singerman Applied Chemistry Division Annapolis, Maryland 21401	1
Dr. William Tolles Superintendent Chemistry Division, Code 6100 Naval Research Laboratory Washington, D.C. 20375-5000	1
Dr. David Young Code 334 NORDA NSTL, Mississippi 39529	1
Naval Weapons Center Attn: Dr. Ron Atkins Chemistry Division China Lake, California 93555	1
Scientific Advisor Commandant of the Marine Corps Code RD-1 Washington, D.C. 20380	1
U.S. Army Research Office Attn: CRD-AA-IP P.O. Box 12211 Research Triangle Park, NC 27709	1
Mr. John Boyle Materials Branch Naval Ship Engineering Center Philadelphia, Pennsylvania 19112	1
Naval Ocean Systems Center Attn: Dr. S. Yamamoto Marine Sciences Division San Diego, California 91232	1

DL/1113/87/2

ABSTRACTS DISTRIBUTION LIST, 056/625/629

Dr. J. E. Jensen
Hughes Research Laboratory
3011 Malibu Canyon Road
Malibu, California 90265

Dr. J. H. Weaver
Department of Chemical Engineering
and Materials Science
University of Minnesota
Minneapolis, Minnesota 55455

Dr. A. Reisman
Microelectronics Center of North Carolina
Research Triangle Park, North Carolina
27709

Dr. M. Grunze
Laboratory for Surface Science
and Technology
University of Maine
Orono, Maine 04469

Dr. J. Butler
Naval Research Laboratory
Code 6115
Washington D.C. 20375-5000

Dr. L. Interante
Chemistry Department
Rensselaer Polytechnic Institute
Troy, New York 12181

Dr. Irvin Heard
Chemistry and Physics Department
Lincoln University
Lincoln University, Pennsylvania 19352

Dr. K. J. Klaubunde
Department of Chemistry
Kansas State University
Manhattan, Kansas 66506

Dr. C. B. Harris
Department of Chemistry
University of California
Berkeley, California 94720

Dr. R. Bruce King
Department of Chemistry
University of Georgia
Athens, Georgia 30602

Dr. R. Reeves
Chemistry Department
Renssaeler Polytechnic Institute
Troy, New York 12181

Dr. Steven M. George
Stanford University
Department of Chemistry
Stanford, CA 94305

Dr. Mark Johnson
Yale University
Department of Chemistry
New Haven, CT 06511-8118

Dr. W. Knauer
Hughes Research Laboratory
3011 Malibu Canyon Road
Malibu, California 90265

Dr. Theodore E. Madey
Surface Chemistry Section
Department of Commerce
National Bureau of Standards
Washington, D.C. 20234

Dr. J. E. Demuth
IBM Corporation
Thomas J. Watson Research Center
P.O. Box 218
Yorktown Heights, New York 10598

Dr. M. G. Lagally
Department of Metallurgical
and Mining Engineering
University of Wisconsin
Madison, Wisconsin 53706

Dr. R. P. Van Duyne
Chemistry Department
Northwestern University
Evanston, Illinois 60637

Dr. J. M. White
Department of Chemistry
University of Texas
Austin, Texas 78712

Dr. Richard J. Saykally
Department of Chemistry
University of California
Berkeley, California 94720

ABSTRACTS DISTRIBUTION LIST, 056/625/629

Dr. F. Carter
Code 6170
Naval Research Laboratory
Washington, D.C. 20375-5000

Dr. Richard Colton
Code 6170
Naval Research Laboratory
Washington, D.C. 20375-5000

Dr. Dan Pierce
National Bureau of Standards
Optical Physics Division
Washington, D.C. 20234

Dr. R. G. Wallis
Department of Physics
University of California
Irvine, California 92664

Dr. D. Ramaker
Chemistry Department
George Washington University
Washington, D.C. 20052

Dr. J. C. Hemminger
Chemistry Department
University of California
Irvine, California 92717

Dr. T. F. George
Chemistry Department
University of Rochester
Rochester, New York 14627

Dr. G. Rubloff
IBM
Thomas J. Watson Research Center
P.O. Box 218
Yorktown Heights, New York 10598

Dr. J. Baldeschwieler
Department of Chemistry and
Chemical Engineering
California Institute of Technology
Pasadena, California 91125

Dr. Galen D. Stucky
Chemistry Department
University of California
Santa Barbara, CA 93106

Dr. A. Steckl
Department of Electrical and
Systems Engineering
Rensselaer Polytechnic Institute
Troy, New York 12181

Dr. John T. Yates
Department of Chemistry
University of Pittsburgh
Pittsburgh, Pennsylvania 15260

Dr. R. Stanley Williams
Department of Chemistry
University of California
Los Angeles, California 90024

Dr. R. P. Messmer
Materials Characterization Lab.
General Electric Company
Schenectady, New York 22217

Dr. J. T. Keiser
Department of Chemistry
University of Richmond
Richmond, Virginia 23173

Dr. R. W. Plummer
Department of Physics
University of Pennsylvania
Philadelphia, Pennsylvania 19104

Dr. E. Yeager
Department of Chemistry
Case Western Reserve University
Cleveland, Ohio 41106

Dr. N. Winograd
Department of Chemistry
Pennsylvania State University
University Park, Pennsylvania 16802

Dr. Roald Hoffmann
Department of Chemistry
Cornell University
Ithaca, New York 14853

Dr. Robert L. Whetten
Department of Chemistry
University of California
Los Angeles, CA 90024

Dr. Daniel M. Neumark
Department of Chemistry
University of California
Berkeley, CA 94720

Dr. G. H. Morrison
Department of Chemistry
Cornell University
Ithaca, New York 14853

DL/1113/87/2

ABSTRACTS DISTRIBUTION LIST, 056/625/629

Dr. G. A. Somorjai
Department of Chemistry
University of California
Berkeley, California 94720

Dr. J. Murday
Naval Research Laboratory
Code 6170
Washington, D.C. 20375-5000

Dr. W. T. Peria
Electrical Engineering Department
University of Minnesota
Minneapolis, Minnesota 55455

Dr. Keith H. Johnson
Department of Metallurgy and
Materials Science
Massachusetts Institute of Technology
Cambridge, Massachusetts 02139

Dr. S. Sibener
Department of Chemistry
James Franck Institute
5640 Ellis Avenue
Chicago, Illinois 60637

Dr. Arold Green
Quantum Surface Dynamics Branch
Code 3817
Naval Weapons Center
China Lake, California 93555

Dr. A. Wold
Department of Chemistry
Brown University
Providence, Rhode Island 02912

Dr. S. L. Bernasek
Department of Chemistry
Princeton University
Princeton, New Jersey 08544

Dr. W. Kohn
Department of Physics
University of California, San Diego
La Jolla, California 92037

Dr. Stephen D. Kevan
Physics Department
University Of Oregan
Eugene, Oregon 97403

Dr. David M. Walba
Department of Chemistry
University of Colorado
Boulder, CO 80309-0215

Dr. L. Kesmodel
Department of Physics
Indiana University
Bloomington, Indiana 47403

Dr. K. C. Janda
University of Pittsburg
Chemistry Building
Pittsburg, PA 15260

Dr. E. A. Irene
Department of Chemistry
University of North Carolina
Chapel Hill, North Carolina 27514

Dr. Adam Heller
Bell Laboratories
Murray Hill, New Jersey 07974

Dr. Martin Fleischmann
Department of Chemistry
University of Southampton
Southampton SO9 5NH
UNITED KINGDOM

Dr. H. Tachikawa
Chemistry Department
Jackson State University
Jackson, Mississippi 39217

Dr. John W. Wilkins
Cornell University
Laboratory of Atomic and
Solid State Physics
Ithaca, New York 14853

Dr. Ronald Lee
R301
Naval Surface Weapons Center
White Oak
Silver Spring, Maryland 20910

Dr. Robert Gomer
Department of Chemistry
James Franck Institute
5640 Ellis Avenue
Chicago, Illinois 60637

Dr. Horia Metiu
Chemistry Department
University of California
Santa Barbara, California 93106

Dr. W. Goddard
Department of Chemistry and Chemical
Engineering
California Institute of Technology
Pasadena, California 91125